Proc Indian Natn Sci Acad **81** No. 1 February 2015 Special Issue, pp. 100-106

DOI: 10.16943/ptinsa/2015/v81i1/48057

Multiple Freezeout

SANDEEP CHATTERJEE*

School of Physical Sciences, National Institute of Science Education and Research, Bhubaneshwar 751 005, *India*

(Received on 1 May 2014; Accepted on 23 June 2014)

The effect of hadrochemistry has largely been ignored while constructing the chemical freezeout stage of the fireball evolution in heavy ion collisions. Thus, almost all models of hadron production use a single chemical freezeout surface where the yields of all hadrons get fixed together. We argue from the viewpoint of hadrochemistry that such a scheme of chemical freezeout should be replaced by a multiple freezeout scheme where mainly hadrons with zero and non-zero strangeness content freezeout separately. This is shown to improve the fits to measured hadron yields in the entire range of $\sqrt{s_{NN}}$ from $6.27 - 2700$ GeV. We also point out possible influence of the QCD critical point and crossover transition on the extracted thermal parameters.

Key Words : Heavy-ion Collision; Chemical Freezeout; Critical Point

Introduction

Hadron resonance gas (HRG) models have been quite successful in describing the hadron yields measured in heavy ion collisions across a large range of centre of mass energy $\sqrt{s_{\rm NN}}$ spanning from the lowest AGS to the topmost RHIC energy of 2.7 - 200 GeV (Braun-Munzinger *et al*., 1996; Yen and Gorenstein, 1999; Becattini *et al*., 2001). Over the last few decades, the following picture for the late stage evolution of the fireball has emerged: First, the chemical composition of the fireball gets fixed. This is known as chemical freezeout (CFO). One of the successful outcomes from such a programme has been the establishment of the CFO surface. A little later, as the mean free path of the hadrons becomes too large to cope up with the fireball expansion, thermal/kinetic freezeout (KFO) takes place when the hadrons stop colliding even elastically. This is when the transverse momentum spectra of the observed particles gets fixed.

*Author for Correspondence : E-mail: chatterjee.sandeep@niser.ac.in

Recently, with the advent of the LHC data there has been a renewed interest in the physics of the CFO. Here we will present our view on the same. QCD has three conserved charges: baryon number B, strangeness S and electric charge Q. Thus, in a heavy ion collision, the thermodynamic state of the strongly interacting fireball in thermal and chemical equilibrium within a grand canonical ensemble can be stated in terms of four thermal parameters: temperature T, baryon chemical potential μ_B, strangeness chemical potential μ_S and electric charge chemical potential μ_Q. Out of these four parameters two can be consistently fixed through the following constraints

$$\text{Net S} = 0 \tag{1}$$

$$\text{Net B / Net Q} = 2.5 \tag{2}$$

The usual practice is to fix μ_S and μ_Q from Eqs. 1 and 2 respectively and fit μ_B and T from data. This is how the CFO surface $\left(\mu_B\left(\sqrt{s_{\rm NN}}\right),\, T\left(\sqrt{s_{\rm NN}}\right)\right)$ is established by fitting data at different $\sqrt{s_{\rm NN}}$.

Model

The fireball in the late stage during CFO is viewed as an ideal relativistic gas of hadrons. This is the HRG phase, the partition function Z in the grand canonical ensemble at a particular beam energy $\sqrt{s_{\rm NN}}$ being given by a sum over all the individual hadron partition function Z_i

$$\log\left[Z\left(\sqrt{s_{\rm NN}}\right)\right] = \sum_i \log\left[Z_i\left(T_i\left(\sqrt{s_{\rm NN}}\right), \mu_i\left(\sqrt{s_{\rm NN}}\right), V_i\left(\sqrt{s_{\rm NN}}\right)\right)\right] \tag{3}$$

The primordial yield $N_i^{\rm p}$ of the ith hadron is obtained by a partial derivative of $\log[Z]$ with respect to its corresponding chemical potential μ_i

$$\begin{aligned} N_i^{\rm p} &= \frac{\partial}{\partial\left(\frac{\mu_i}{T_i}\right)}\log[Z] \\ &= \frac{V_i T_i}{\pi^2} g_i m_i^2 \sum_{l=1}^{\infty} (-a)^{l+1}\, l^{-1} K_2\left(l m_i / T_i\right) \\ &\times \exp\left(l\left(B_i \mu_{B_i} + Q_i \mu_{Q_i} + S_i \mu_{S_i}\right)/T_i\right) \end{aligned} \tag{4}$$

where $a = -1$ for bosons and 1 for fermions. m_i and g_i are the mass and degeneracy factors of the ith hadron respectively and B_i, Q_i and S_i are its conserved charges. K_2 is the Bessel function of the second kind. In order to compare with experimental data of the hadron yields, we need to take into account of the decay contribution from resonances

$$N_i^{\rm t} = N_i^{\rm p} + \sum_j N_j^{\rm p} \times \text{B.R.}_{j\to i} \tag{5}$$

Here N_i^{t} is the sum of primordial as well as feeddown from heavier resonances and B.R.$_{j\to i}$ is the branching ratio of the channel in which the jth hadron decays to the ith hadron taken from P.D.G. (Beringer *et al.*, 2012).

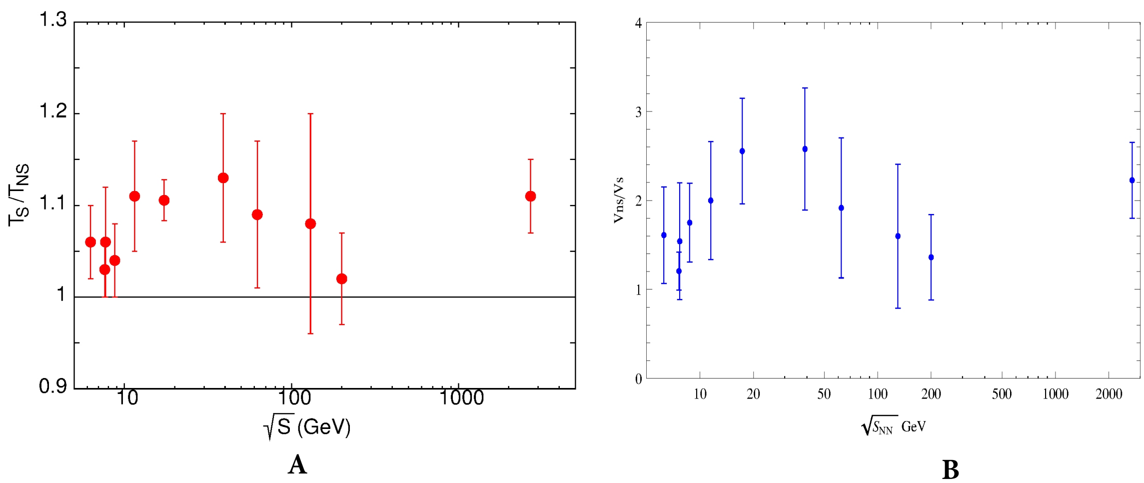

Fig. 1: The ratio of temperatures in red (A) and volumes in blue (B) from the two surfaces. Non-monotonic variation with a hint of a broad peak in the energy range $\sqrt{s_{\mathrm{NN}}} \sim 10-40$ GeV is observed. The left hand side figure is taken from Ref. (Chatterjee *et al.*, 2013)

The standard practice is to assume a single CFO surface (1CFO) where the yields of all the hadrons get fixed. Hence in Eq. 3, $T_i\left(\sqrt{s_{\mathrm{NN}}}\right) = T\left(\sqrt{s_{\mathrm{NN}}}\right)$ for all hadrons. Similarly, V_i, μ_{B_i}, μ_{Q_i} and μ_{S_i} are same for all hadrons. Such a scheme has been quite successful in describing the hadron multiplicities across a broad range of energies with a few exceptions, the most notable being the LHC energy of $\sqrt{s_{\mathrm{NN}}} = 2700$ GeV. Ever since there has been the report of proton anomaly at LHC (Abelev *et al.*, 2012; Rybczynski *et al.*, 2012; Andronic *et al.*, 2013), a lot of new alternatives to the above standard CFO mechanism has been proposed. There have been efforts to include late stage inelastic scatterings through a hadronic afterburner based on URQMD model (Steinheimer *et al.*, 2013, Becattini *et al.*, 2013, 2012) post 1CFO that mainly lead to proton-antiproton anihilations. Attempts have been also made to include nonequlibrium parameters as additional fit parameters to the standard 1CFO scheme to expain the yields (Petran *et al.*, 2013). Here we will discuss a recent proposal to extend the standard 1CFO scheme to multiple freezeout scenarios that can also successfully address the above anomaly (Chatterjee *et al.*, 2013; Bugaev *et al.*, 2013). The multitude of interactions that are going on in the fireball in the proximity of the CFO can be broadly classfied into two categories based on energetics: (a) Those mediated by kaons that typically involve higher energy thresholds compared to T, for example, $p + K \leftrightarrow \Lambda + X$, $\Lambda + K \leftrightarrow \Xi + X$ (X is the appropriate daughter hadron) etc., and (b) Those mediated by pions that typically involve lower energy thresholds as compared to the

$\sqrt{S_{NN}}$ (GeV)	$10^4 V_S$ (MeV^{-3})	$10^4 V_{NS}$ (MeV^{-3})	T_S (MeV)	T_{NS} (MeV)	μ_S (MeV)	μ_{NS} (MeV)	χ^2/N_{df}
6.27	1.1 (0.2)	1.6 (0.3)	139 (4)	131 (4)	435 (11)	446 (10)	1.6/4
7.62	1.2 (0.2)	1.4 (0.3)	144 (3)	139 (3)	399 (13)	395 (10)	3.0/5
7.7	1.0 (0.2)	1.5 (0.6)	147 (3)	138 (8)	424 (18)	368 (28)	8.0/4
8.76	0.8 (0.1)	1.3 (0.4)	152 (3)	145 (5)	393 (15)	358 (18)	4.4/5
11.5	1.0 (0.1)	1.9 (0.7)	157 (3)	142 (7)	310 (15)	278 (28)	0.8/4
17.3	1.1 (0.2)	2.8 (0.4)	157 (3)	142 (3)	214 (14)	208 (8)	15/7
39.	1.0 (0.2)	2.4 (0.8)	168 (4)	148 (8)	115 (13)	98 (24)	1.2/4
62.4	1.3 (0.3)	2.3 (0.7)	169 (5)	155 (8)	70 (20)	65 (25)	8.0/7
130.	1.6 (0.5)	2.5 (1.0)	169 (6)	157 (8)	35 (23)	25 (20)	4.4/5
200.	2.2 (0.4)	2.8 (0.8)	164 (3)	155 (6)	31 (11)	22 (16)	23/6
2700.	4.1 (0.6)	8.8 (0.8)	162 (3)	146 (3)	14 (12)	-2 (7)	4.4/6

Table 1: **The freezeout parameters in 2CFO; the errors indicated are for single parameter variation (Chatterjee** ***et al*****., 2013)**

ambient T like $p + \pi \leftrightarrow n + \pi$ (Kitazawa and Asakawa, 2012; Chatterjee *et al*., 2013). Thus because of higher energy threshold (and also the fact that the kaon density is at any instant much lower than that of pion) we expect those with non zero strangeness content to chemically freezeout earlier as compared to those with zero strangeness content (2CFO). Thus in Eq. 3 $T_i = T_{\rm s}$ for all strange hadrons and those with hidden strangeness content while $T_i = T_{\rm ns}$ for all the rest of the non strange hadrons. We treat the volume and chemical potentials also similarly. Within such a 2CFO scheme hadron yields were fitted and thermal parameters extracted for $\sqrt{s_{\rm NN}} = 6.27 - 2700$ GeV (Chatterjee *et al*., 2013).

Result

The thermal parameters characterising the strange and non strange CFO surfaces as extracted from fits to hadron yields in 2CFO are given in Table 1. It is interesting to note that for all beam energies, $T_{\rm s} > T_{\rm ns}$ and consequently $V_{\rm s} < V_{\rm ns}$. This confirms our picture of an expanding fireball where the strange hadrons first freezeout followed by the non strange hadrons at a later time.

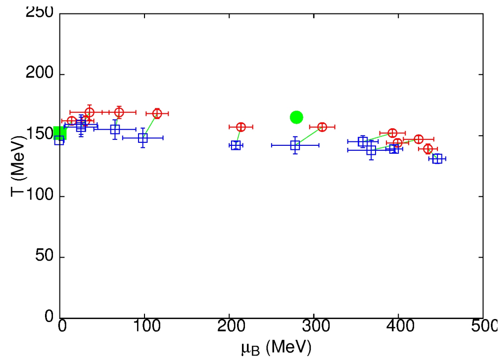

Fig. 2: The freezeout points for 2CFO on the phase diagram (circles: strange, squares: non-strange). Points from the same $\sqrt{s_{\rm NN}}$ are joined by lines. The filled square is the predicted position of the QCD crossover at $\mu = 0$ (Aoki *et al*., 2009) and the filled circle of the QCD critical point (Gavai and Gupta, 2008). The figure is taken from Ref. (Chatterjee *et al*., 2013)

In Fig. 1 we have plotted the two ratios, $T_{\rm s}/T_{\rm ns}$ and $V_{\rm ns}/V_{\rm s}$ with $\sqrt{s_{\rm NN}}$. Both the ratios show similar non monotonic features- an initial rise followed by a hint of a peak like structure in the intermediate energy range between 10-40 GeV and then a fall upto top RHIC energy of 200 GeV. There is again a rise at the LHC energy of 2700 GeV. Let us now turn our attention to Fig. 2. Here we have plotted the strange and non strange CFO surfaces on the QCD phase diagram and also labelled the probable locations of the QCD critical point (Gavai and Gupta, 2008) and the QCD crossover at zero baryon chemical potential (Aoki *et al*., 2009). A close simultaneous inspection of Figs. 1 and 2 seem to suggest that the ratios $T_{\rm s}/T_{\rm ns}$ and $V_{\rm ns}/V_{\rm s}$ seem to peak near the above mentioned lattice QCD predicted points thus signalling a separation of the CFO surfaces near the QCD critical point and crossover transitions. A possible explanation at the LHC energy could be that between the two CFOs the fireball passes close to the QCD chiral crossover point. This is in the critical region of the chiral transition in a theory with $m_\pi = 0$ (Ejiri *et al*., 2009). The freezeout points for 2CFO on the phase diagram (circles: strange, squares: non-strange). Points from the same $\sqrt{s_{\rm NN}}$ are joined by lines. The filled square is the predicted position of the QCD crossover at $\mu = 0$ (Aoki *et al*., 2009) and the filled circle of the QCD critical point (Gavai and Gupta, 2008). The figure is taken from Ref. (Chatterjee *et al*., 2013). Thus chiral critical behaviour may then delay pion CFO by lowering the scalar mass. However, for a clearer picture, data from higher energy runs at the LHC will be crucial as the system will get closer to the $\mu_B = 0$ axis with increasing $\sqrt{S}$. Now let us focus in the intermediate energies of $\sqrt{s_{\rm NN}} \sim 10-40$ GeV where we observe a broad peak in Fig. 1. The comparison of fireball evolution trajectories at $\sqrt{s_{\rm NN}} = 11.3$ and 17.3 GeV (see Fig. 2) indicate a focusing of trajectories- hydrodynamic anomalies of this kind are expected when system passes near a critical point (Stephanov *et al*., 1998). Thus the broad peak in the ratios shown in Fig. 1 could be due to a delay in the CFOs, possibly a slow expansion in out-of-equilibrium dynamics near the critical point, followed by re-thermalization and delayed freezeout. All these call for a long enough run in this region of $\sqrt{s_{\rm NN}}$ so that one has enough statistics to study hadron yields more precisely.

Conclusion

It was argued on the basis of hadrochemistry there could be more details in the chemical freezeout stage of the fireball evolution than currently implemented in the analysis of the hadron yields via an ideal hadron resonance gas model. As a first step, the standard scenario of a single chemical freezeout surface has been extended to a double freezeout surfaces scheme where those hadrons with zero strangeness content freeze-out separately as compared to those with non-zero strangeness content. This simplest multiple freezeout scenario was implemented and thermal parameters extracted from fits to hadron yields across $\sqrt{s_{\rm NN}}$ from $6.27 - 2700$ GeV. The fitted parameters allow us to draw a consistent picture of fireball evolution in the chemical freezeout stage where the strange hadrons freezeout earlier followed by the non strange ones at all energies. Non monotonic variations, although with large errors, of certain combinations of the thermal parameters eg. $T_{\rm s}/T_{\rm ns}$ and $V_{\rm ns}/V_{\rm s}$ were observed and their possible connections with the QCD critical point and crossover transitions were mentioned.

Acknowledgement

I would like to acknowledge helpful discussions and collaboration on this subject with Rohini Godbole and Sourendu Gupta. I also acknowledge financial support from DST SwarnaJayanti project of Dr. Bedangadas Mohanty.

References

1. Abelev B *et al.* (ALICE Collaboration) (2012) Pion, Kaon, and Proton Production in Central Pb–Pb Collisions at $\sqrt{s_{NN}}$=2.76 TeV *Phys Rev Lett* **109** 252301.
2. Andronic A, Braun-Munzinger P, Redlich K and Stachel J (2013) The statistical model in Pb-Pb collisions at the LHC *Nucl Phys* **A904-905** 535c
3. Aoki Y *et al.* (2009) The QCD transition temperature: results with physical masses in the continuum limit II *JHEP* **06** 088
4. Becattini F, Cleymans J, Keranen A, Suhonen E and Redlich K (2001) Features of particle multiplicities and strangeness production in central heavy ion collisions between 1.7A-GeV/c and 158A-GeV/c *Phys Rev* **C64** 024901
5. Becattini F *et al.* (2013) Hadron Formation in Relativistic Nuclear Collisions and the QCD Phase Diagram *Phys Rev Lett* **111** 082302
6. Becattini F *et al.* (2012) Hadronization and Hadronic Freeze-Out in Relativistic Nuclear Collisions *Phys Rev* **C85** 044921
7. Beringer J *et al.* (Particle Data Group) (2012) Review of Particle Physics *Phys Rev* **D86** 010001
8. Braun-Munzinger P, Stachel J, Wessels J and Xu N (1996) Thermal and hadrochemical equilibration in nucleus-nucleus collisions at the SPS *Phys Lett* **B365** 1

9. Bugaev K *et al.* (2013) Chemical Freeze-out of Strange Particles and Possible Root of Strangeness Suppression *Europhys Lett* **104** 22002
10. Chatterjee S, Godbole R and Gupta S (2013) Strange freezeout *Phys Lett* **B727** 554
11. Ejiri S *et al.* (2009) On the magnetic equation of state in (2+1)-flavor QCD *Phys Rev* **D80** 094505
12. Gavai R and Gupta S (2008) QCD at finite chemical potential with six time slices *Phys Rev* **D78** 114503
13. Kitazawa M and Asakawa M (2012) Revealing baryon number fluctuations from proton number fluctuations in relativistic heavy ion collisions *Phys Rev* **C85** 021901
14. Petran M, Letessier J, Petracek V and Rafelski J (2013) Hadron production and quark-gluon plasma hadronization in Pb-Pb collisions at $\sqrt{s_{NN}}$=2.76 TeV *Phys Rev* **C88** 034907
15. Rybczynski M, Florkowski W and Broniowski W (2012) Single-freeze-out model for ultra relativistic heavy-ion collisions at $\sqrt{s_{NN}}$=2.76 TeV and the LHC proton puzzle *Phys Rev* **C85** 054907
16. Steinheimer J, Aichelin J and Bleicher M (2013) Non-thermal p/π ratio at LHC as a consequence of hadronic final state interactions *Phys Rev Lett* **110** 042501
17. Stephanov MA, Rajagopal K and Shuryak EV (1998) Signatures of the tricritical point in QCD *Phys Rev Lett* **81** 4816
18. Yen GD and Gorenstein MI (1999) The Analysis of particle multiplicities in Pb + Pb collisions at CERN SPS within hadron gas models *Phys Rev* **C59** 2788.